Modular Construction of Photoanodes with Covalently Bonded Ru- and Ir-Polypyridyl Visible Light Chromophores

Journal:	*ACS Applied Materials & Interfaces*
Manuscript ID	am-2018-06605q.R1
Manuscript Type:	Article
Date Submitted by the Author:	21-Jun-2018
Complete List of Authors:	Wang, Chao; University of Alberta, Chemistry Amiri, Mona; University of Alberta, Department of Chemistry Endean, Riley; University of Alberta, Chemistry Martinez Perez, Octavio; University of Alberta, Chemistry Varley, Samuel; University of Alberta Department of Chemistry Rennie, Ben; University of Alberta, Chemistry Rasu, Loorthuraja; University of Alberta, Department of Chemistry Bergens, Steven; University of Alberta, Department of Chemistry, Steven Bergens

Modular Construction of Photoanodes with Covalently Bonded Ru- and Ir-Polypyridyl Visible Light Chromophores

*Chao Wang, Mona Amiri, Riley T. Endean, Octavio Martinez Perez, Samuel Varley, Ben Rennie, Loorthuraja Rasu, and Steven H. Bergens**

Department of Chemistry, University of Alberta, 11227 Saskatchewan Drive, Edmonton, Alberta T6G 2G2, Canada.

KEYWORDS ruthenium polypyridyl complex, iridium polypyridyl complex, diazonium, electrografting, photoelectrochemistry, photoanode, visible light chromophore.

ABSTRACT 1,10-phenanthroline is grafted to indium tin oxide (ITO) and titanium dioxide nanoparticle (TiO_2) semiconductors by electroreduction of 5-diazo-1,10-phenanthroline in 0.1 M H_2SO_4. The lower and upper potential limits (-0.20 and 0.15 V_{SCE}, respectively) were set to avoid reduction and oxidation of the 1,10-phenanthroline (phen) covalently grafted at C5 to the semiconductor. The resulting semiconductor-phen ligand (ITO-phen or TiO_2-phen) was air stable, and was bonded to Ru- or Ir- by reaction with *cis*-$[Ru(bpy)_2(CH_3CN)_2]^{2+}$ (bpy = 2,2'-bipyridine) or *cis*-$[Ir(ppy)_2(CH_3CN)_2]^{+}$ (ppy = *ortho*-C_{phenyl} metallated 2-phenylpyridine) in CH_2Cl_2 and THF solvent at 50 °C. Cyclic voltammetry, X-ray photoelectron spectroscopy, solid-state UV-vis, and

inductively coupled plasma mass spectrometry all confirmed that the chromophores SC-$[(phen)Ru(bpy)_2]^{2+}$ and SC-$[(phen)Ir(ppy)_2]^{+}$ (SC = ITO or TiO_2) formed in near quantitative yields by these reactions. The resulting photoanodes were active and relatively stable to photoelectrochemical oxidation of hydroquinone and triethylamine under neutral and basic conditions.

INTRODUCTION

We report the modular, versatile assembly of relatively base-stable photoanodes by covalent bonding of $[(phen)Ru(bpy)_2]^{2+}$ (bpy = 2,2'-bipyridine, phen = 1,10-phenanthroline) or *cis*-$[(phen)Ir(ppy)_2]^{+}$ (ppy = *ortho*-C_{phenyl} metallated 2-phenylpyridine) to various metal oxide semiconductors (SC). Solar energy is essentially unlimited, and can meet most of our future energy demands with minimal negative impact on the environment.[1-2] Cost-effective, efficient, and rapid large-scale storage is an inescapable requirement of the wide-spread utilization of renewable energy.[3] Solar energy can be stored with the water oxidation reaction (WOR) by converting the protons and electrons into H_2, or by using them to reduce carbon dioxide to form reusable fuels.[4-5] In 1972, Fujishima and Honda reported the first photoelectrochemical conversion of water into H_2 and O_2. This water splitting reaction (WSR) utilized TiO_2 as the semiconductor/catalyst and UV illumination as the energy source.[6] Visible light constitutes ~44% of the solar spectrum,[7] and several approaches are being pursued to develop efficient visible light-driven WSR systems.[5,8-10] For example, narrow band-gap semiconductors including WO_3,[11] $BiVO_4$,[10,12] $SrTiO_3$,[13-14] and doped TiO_2,[15] are being investigated as visible light-driven photoelectrodes. Dye-sensitized photoelectrochemical cells (DSPECs) typically contain well-defined, separate photosensitizers (chromophores) and electrocatalysts. This distribution of

function allows for independent optimization, and for direct study of their roles and interactions within operating DSPECs.[16-18]

Ru- and Ir-polypyridyl complexes are common chromophores utilized in photoelectrochemical applications because they have strong, tunable metal-to-ligand charge transfer absorbance. They also undergo efficient intersystem crossing, and their excited states have relatively long lifetimes.[19] Ruthenium is more abundant than iridium, and Ru(II)-polypyridine complexes have wide absorption ranges that extend into the visible, and near infrared regions of the solar spectrum.[20-22] The first report of visible light WSR DSPEC was in 2009 by Mallouk's group.[23] Their photoanode utilized Ru(II)(4,4'-dimethyl-bpy)(4,4'-$(PO_3H_2)_2$-bpy)(4-methyl-4'-$CH(COOH)_2$-bpy) as the chromophore (loading = 3.2×10^{-8} mol cm^{-2}), and IrO_2 as the WOR catalyst adsorbed onto TiO_2. Hydrogen was produced at a Pt cathode. The visible-light driven WSR current density reached 0.03 mA cm^{-2} (0 V_{SCE} bias, Xenon lamp, > 410 nm, pH 5.75 Na_2SiF_6-$NaHCO_3$ buffer). To date, the most active DSPEC for visible-light driven WSR was constructed by Sun's group utilizing $[Ru(II)(bpy)_2(4,4'\text{-}(PO_3H_2)_2\text{-}bpy)]^{2+}$ as the chromophore, and Ru(II)(bda)(4-picoline)L (H_2bda = bipyridine-dicarboxylic acid; L = *N*-(3-(triethoxysilyl)propyl)isonicotinamide) as the water oxidation catalyst adsorbed onto TiO_2. The visible-light driven WSR current density reached 1.7 mA cm^{-2} (-0.04 V_{SCE} bias, 300 mW cm^{-2} Xenon lamp, > 410 nm, pH 6.8 phosphate buffer, 2.51×10^{-9} mol cm^{-2} chromophore, 8.38×10^{-10} mol cm^{-2} WOR catalyst, Pt cathode).[24] Meyer's group has reported the Ru(II) polypyridyl-based covalent chromophore-catalyst assembly, $[(4,4'\text{-}(PO_3H_2)_2\text{-}bpy)_2Ru(4\text{-}Mebpy\text{-}4'\text{-}epic)Ru(bda)(4\text{-}picoline)]^{2+}$ (4-Mebpy-4'-epic = 4-(4-methylbipyridin-4'-yl-ethyl)-pyridine), adsorbed on a SnO_2/TiO_2 core–shell electrode. The visible-light driven WSR current density reached 0.85 mA cm^{-2} (0.05 V_{SCE} bias, 100 mW cm^{-2} white light, pH 5.7 acetate buffer, Pt cathode).[25]

The WSR photocurrent of DSPECs often decays from desorption of the chromophore and/or catalyst into water.[4,26] For non-aqueous applications, Ru and Ir chromophores have been deposited by methods including spin coating,[27] Langmuir-Blodgett films,[28] self-assembly of monolayers,[29] and diazonium electroreduction.[30-32] For aqueous environments, Ru chromophores are commonly attached to semiconductors through phosphonate, or carboxylate ester bonds made by condensation between semiconductor surface hydroxides and acid groups attached to ligands in the chromophore.[4,23-24,33] These chromophores typically suffer from desorption under basic conditions through hydrolysis of the esters.[34-36] Atomic layer deposition (ALD) of Al_2O_3 or TiO_2 layers improves the stability of chromophore-WOR catalyst/semiconductor layers.[37-38] Silatrane and hydroxamic acid anchoring groups have also been utilized as binders, providing enhanced stability towards hydrolysis up to pH 11.[39-41]

The rate of the WOR typically increases with pH.[16] As well, a wide variety of earth abundant catalysts are stable under alkaline conditions, but dissolve in acid.[42] Moreover, proton reduction is less competitive with CO_2 reduction at higher pHs.[43] For these reasons, it is necessary to develop anchoring/protection methods that stabilize chemical linkages between chromophore- or catalyst molecules and metal oxide semiconductors in strong alkaline solutions.[16] Electroreduction of aryl diazonium ions forms aryl radicals that have been covalently grafted to a variety of surfaces including metals, metal oxides, and carbon.[44-46] The direct grafting of diazonium-modified organometallic precursors to several electrode surfaces has been reported.[30-32,45,47] For example, Meyer et al. grafted a Ru(II) diazonium-modified chromophore to a TiO_2 electrode. The resulting photoanode was more stable under alkaline conditions (0.1 M acetate buffer with 0.5 M $NaClO_4$ and 0.05 M triethanolamine, pH 12) than phosphonic ester linkages.[48]

This approach requires excess organometallic-diazonium compound that cannot be reused, and the lifetime of the radical intermediate depends upon the nature of the compound.[44]

We report a convenient and reliable covalent grafting of 1,10-phenanthroline (phen) at C5 to indium-doped tin oxide (ITO) and titanium dioxide (TiO_2) surfaces by diazonium electroreduction. The resulting semiconductor-phen ligand (SC-phen) bonds to Ru- and Ir-organometallic precursors forming the corresponding chromophores (Scheme 1).

EXPERIMENTAL SECTION

Materials. Chemicals were used without purification unless noted otherwise; 1,10-phenanthroline-5-amine (Sigma Aldrich, 97%), H_2SO_4 (Sigma Aldrich, 99.999%), anhydrous ethanol (Commercial Alcohols), $NaNO_2$ (Sigma Aldrich, ≥ 97.0%), dichloromethane, distilled (Sigma Aldrich, ACS reagent, ≥ 99.5%), NH_4OH (Caledon), TiO_2 nanoparticles (Sigma Aldrich, anatase, nanopowder < 25 nm particle size, 99.7% trace metals basis), Triton X-100 (EMD Millipore Corporation), 2,4-pentanedione (Sigma Aldrich, ≥ 99%), tetrahydrofuran, distilled (Sigma Aldrich, ACS reagent, ≥ 99.0%), $TiCl_4$ (Sigma Aldrich, ≥ 99.995%, trace metals basis), $NaClO_4$ (Sigma Aldrich, ACS reagent, ≥ 98.0%), hydroquinone (Sigma Aldrich, ReagentPlus, ≥ 99.5%), triethylamine, distilled (Sigma Aldrich, ≥ 99.0%), Na_2SO_4 (Sigma Aldrich, ACS reagent, ≥ 99.0%),and triply distilled water.

Fabrication of TiO_2 coated FTO electrode. FTO slides (Sigma Aldrich, surface resistivity ~7 Ω/sq) were sonicated in ethanol and water for 30 min each, and then treated in a 50 mM $TiCl_4$ solution at 70 ^oC for 30 min. TiO_2 paste was prepared following reported literature procedure.[49-50] Briefly, 2.0 g TiO_2 nanoparticles were mixed with 200 μL Triton X-100 surfactant and 200 μL 2,4-pentanedione in a 12 ml ethanol/water 1:1 solution, and stirred vigorously for 2 hours,

followed by sonication for 30 min. The paste was doctor-bladed on a FTO surface with 4 layers of scotch tape as spacer. After dried in air, the electrode was heated to 500 ^{o}C for 2 h, followed by immersion in a 50 mM $TiCl_4$ solution at 70 ^{o}C for 30 min, wash with water and ethanol, and heat treatment at 450 ^{o}C for 30 min. Figure S1 shows the morphology and thickness of the TiO_2 film.

Electrograft of 1,10-phenanthroline-5-amine. ITO coated glass slide (Sigma Aldrich, surface resistivity 8-12 Ω/sq) was cut into 2.5 × 1.2 cm^2 rectangular shape, and sonicated 15 min each in 5 ml acetonitrile, 5 ml 2-propanol and 5 ml triply distilled water, then dried under nitrogen flow. Two different electrografting techniques were implemented for deposition of 1,10-phenanthroline; i.e. cyclic voltammetry at different sweep rates and potentiostatic for different durations. However, the optimized method with highest surface coverage was cyclic voltammetry as follows. Electrochemical grafting of 1,10-phenanthroline onto ITO slide (or TiO_2 coated FTO slide) was carried out following previous report.[51] Briefly, 20 ml aqueous 0.1 M H_2SO_4 solution containing 1 mM 5-amino-1,10-phenanthroline (3.9 mg) was purged with N_2 for 15 min. One minute after 2 mM $NaNO_2$ (2.8 mg) was added, ~ 1 cm^2 ITO slide was immersed into the solution as the working electrode. The potential was scanned between 0.15 and -0.20 V vs. saturated calomel reference electrode (SCE) at 50 mV s^{-1} for 10 cycles. After electrochemical modification, the 1,10-phenanthroline coated ITO slide (ITO-phen) was rinsed and sonicated in water for 20 seconds to remove physically absorbed species. The counter electrode was graphite. The 1,10-phenanthroline grafted TiO_2 coated FTO electrode (TiO_2-phen) did not undergo sonication. The ITO-phen (or TiO_2-phen) electrode was rinsed with distilled water and then immersed in a solution of ethanol, and ammonium hydroxide (1:1) for 1 hour to deprotonate the as-deposited phenanthroline. The electrode was then rinsed with water and ethanol, and dried

under air.

Grafting of $[Ir(ppy)_2(CH_3CN)_2]OTf$ or $[Ru(bpy)_2(CH_3CN)_2](OTf)_2$ onto ITO-phen or TiO_2-phen. The $[Ir(ppy)_2(CH_3CN)_2]OTf$ and $[Ru(bpy)_2(CH_3CN)_2](OTf)_2$ are synthesized based on previous reports.[52-53] The electrode was placed in a Schleck tube and purged with nitrogen for 15 minutes. $[Ir(ppy)_2(CH_3CN)_2]OTf$ (20 mg, 0.0260 mmol) or $[Ru(bpy)_2(CH_3CN)_2](OTf)_2$ (20 mg, 0.0252 mmol) was weighed out in the Schlenk tube. 0.5 ml of dichloromethane and 4.5 ml of THF were cannulated to dissolve the solid. The Schlenk tube was immersed in a paraffin oil bath and heated to 50 °C for 2 hours. After cooled down to room temperature, the electrode was removed from the bath and rinsed with CH_2Cl_2 (5 ml) and water (2 ml). The resulting electrodes ITO-$[(phen)Ir(ppy)_2]^+$ and ITO-$[(phen)Ru(bpy)_2]^{2+}$ are stable in air under dark for over six months. The deposition on TiO_2 electrode follows the same procedure, and the resulting electrodes are labeled as TiO_2-$[(phen)Ir(ppy)_2]^+$ and TiO_2-$[(phen)Ru(bpy)_2]^{2+}$, respectively.

Preparation of $[Ru(bpy)_2(4,4'-(PO_3H_2)_2bpy)]^{2+}$ sensitized TiO_2 coated FTO electrodes. The synthesis of $[Ru(bpy)_2(4,4'-(PO_3H_2)_2bpy)]Br_2$ is based on previous report.[54] The TiO_2 coated FTO electrode is dipped in a solution of 10 μM $[Ru(bpy)_2(4,4'-(PO_3H_2)_2bpy)]Br_2$ compound in 0.1 M $HClO_4$ for 12 hours, followed by dipping in 0.1 M $HClO_4$ solution for another 12 hours.[55] The resulting electrode (denoted as RuP-TiO_2) is washed with water, dried, and used.

Photoelectrochemistry. The electrolyte used for photoelectrochemistry studies was a 0.1 M $NaClO_4$ solution containing either 0.5 M triethylamine (pH = 12.6) or 0.02 M hydroquinone (pH = 7.0). The counter electrode was a coiled platinum wire, and the reference electrode was a saturated calomel electrode. The electrolyte was stirred using a magnetic stir bar at 500 rpm. The homemade 100 ml four-neck quartz flask with a flat window was used as the reaction flask for

photoelectrochemical experiments. The solution was purged with argon for 30 minutes prior to each measurement, followed by maintaining Ar atmosphere on top of the solution. Working electrode was washed with distilled water before use. The Newport QEPVSI-b system (300 W Xe lamp with Cornerstone M 260 monochromator) was calibrated against a silicon diode with known IPCE, and was used for incident photon-to-current conversion efficiency (IPCE) measurements. The incident light intensity was also checked with Thorlab S121C light meter. The IPCE was calculated based on the equation 1:

$$\text{IPCE}\ (\%) = \frac{100\times1240\times i}{P\lambda} \qquad (1)$$

where i is the photocurrent density (mA cm^{-2}), P is the light power (mW cm^{-2}), and λ is the wavelength (nm).

Instrumentation. Electrochemical studies were done using Solartron SI 1287 Electrochemical Interface controlled by CorrWare for Windows Version 2-3d software. The X-ray photoelectron spectroscopy (XPS) measurements were performed on a Kratos Axis 165 instrument. The base pressure in the sample analytical chamber (SAC) was lower than 1×10^{-9} torr. A monochromatized Al Kα source (hν =1486.6 eV) was used at 12 mA and 14 kV. Survey scans spanned from the binding energy of 1100 to 0 eV, collecting with an analyzer pass energy of 160 eV and steps at 0.3 eV. Inductively coupled plasma–mass spectrometry (ICP-MS) analyses were performed with Perkin Elmer Elan 6000. The SC-$[(phen)Ru(bpy)_2]^{2+}$ and SC-$[(phen)Ir(ppy)_2]^{+}$ electrodes were dissolved in aqua regia solution for 24 hours to etch the SC layer in order to assess the surface coverage of Ru- or Ir- chromophores. UV-vis spectra were acquired using Cary 400 UV-vis spectroscopy. To acquire UV-vis spectra on SC surface, n pieces of SC-$[(phen)Ru(bpy)_2]^{2+}$ or SC-$[(phen)Ir(ppy)_2]^{+}$ were bonded together to enhance the signal (n = 5 for

ITO and 1 for TiO_2). The spectra shown were the acquired spectra absorbance divided by n, with bare ITO or TiO_2 absorbance deducted.

RESULTS AND DISCUSSION

The electroreduction of in situ generated 5-diazo-1,10-phenanthroline over carbon electrodes was reported by the groups of Ekinci and Bélanger.[51,56] Figure 1A shows the cyclic voltammogram (CV) for the electroreduction of the 5-diazo-1,10-phenanthroline cation over ITO in 0.1 M H_2SO_4 (0.15 to -0.2 V versus SCE, all potentials in this paper are reported versus SCE except in non-aqueous electrolytes, scan rate of 50 mV s^{-1}). As reported for glassy carbon,[51] the first negative going sweep contains a large peak corresponding to reduction of the diazonium ion. This peak decreases with cycling as the active sites are blocked by the deposition.[44] It was reported that phen grafted on glassy carbon undergoes irreversible reductions at potentials below -0.78 V, and oxidations above 0.42 V. A potential window between 0.15 and -0.2 V was chosen to avoid these degradations.

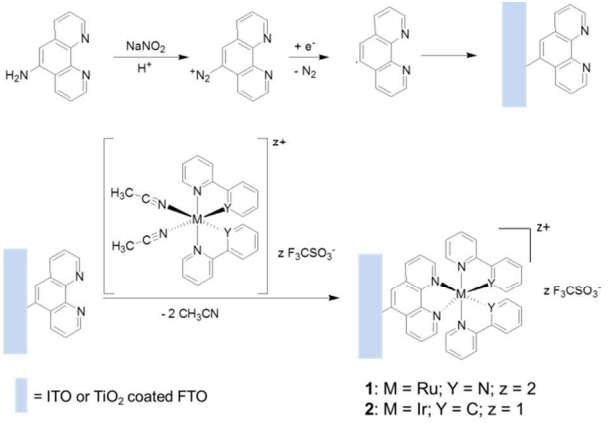

Scheme 1. Illustration of the electrochemical deposition of 5-diazo-1,10-phenanthroline cation, and subsequent formation of semiconductor-chromophore electrode.

Figure 1B shows the high resolution N 1s region XPS spectra of the ITO electrode before and after the diazonium reduction. The N 1s peak at 398.7 eV after grafting indicates the pyridine-type nitrogen, hence presence of phen, on the ITO surface.[57] Figure 1C shows the redox peaks for the redox probe $Fe(CN)_6^{3-/4-}$ (5 mM $K_3[Fe(CN)_6]$) are diminished and separated over ITO-phen compared to bare ITO in CVs recorded in 0.1 M KCl. This inhibition of the electron transfer is also consistent with the presence of phen on the ITO surface. The $Fe(CN)_6^{3-/4-}$ redox peak was not fully suppressed, indicating the film is thin and/or porous.[51]

Figure 1D shows CVs of the ITO-phen and bare ITO electrodes with a strongly reducing lower limit (-0.1 to -1.0 V) in 0.1 M Na_2SO_4. The first negative going sweep with the ITO-phen electrode contained a strong reduction peak at -0.82 V with a shoulder at -0.57 V that was greatly diminished in the second sweep. This response is quite similar to that reported by Bélanger for phen grafted to glassy carbon, and is attributed to $2e^-/2H^+$ reduction forming 1,4-dihydropyridine-type compounds.[51,58] The charge under the reduction peak corresponded to an estimated surface coverage by grafted phen = 2.4×10^{-10} mol cm^{-2}, assuming a two-electron process.

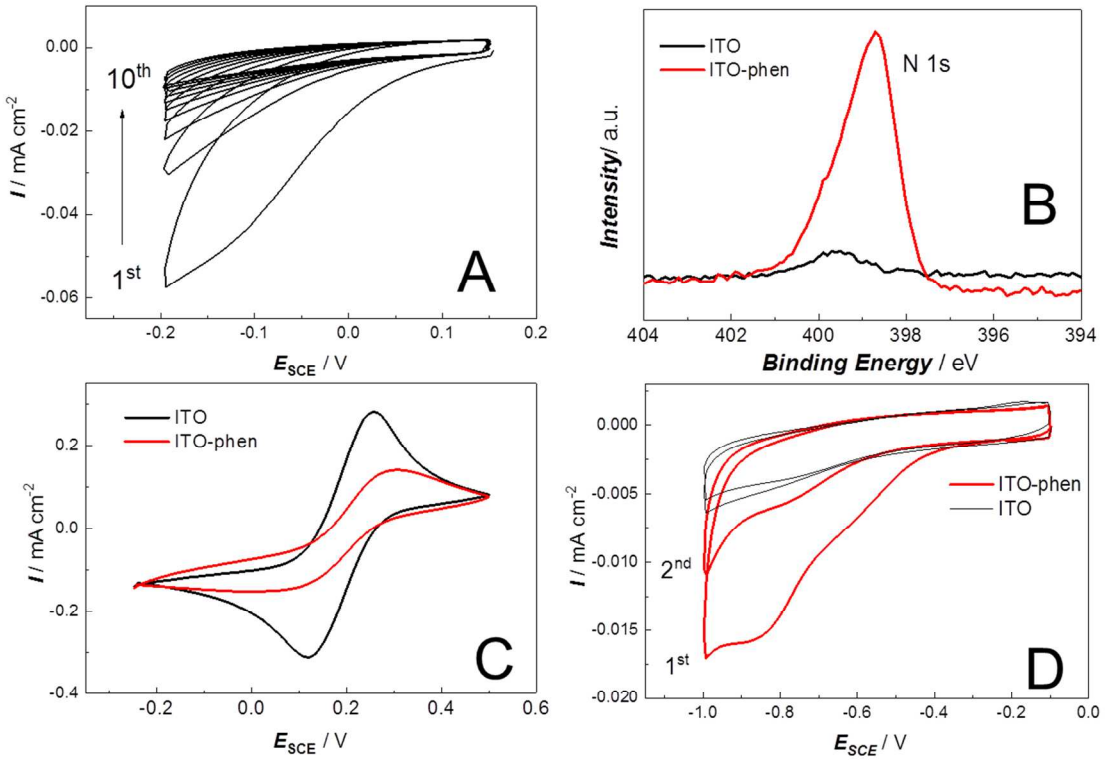

Figure 1. (A) Cyclic voltammogram of the ITO electrode in a 0.1 M H_2SO_4 solution containing 5-amino-1,10-phenanthroline (1 mM) and $NaNO_2$ (2 mM), scan rate 50 mV s^{-1}; (B) High resolution N 1s region XPS spectra of the ITO electrode before and after 1,10-phenanthroline deposition; (C) Cyclic voltammograms for the bare ITO and 1,10-phenanthroline modified ITO electrode in 0.1 M KCl solution containing 5 mM $Fe(CN)_6^{3-}$ at scan rate of 20 mV s^{-1}; (D) Cyclic voltammograms of the ITO-phen and bare ITO electrodes in a N_2-saturated 0.1 M Na_2SO_4 solution and a scan rate of 50 mV s^{-1}.

In principle, the ITO-phen ligand is protonated at nitrogen under the acidic conditions of the electrografting. Indeed, it was necessary to rinse the ITO-phen ligand with aqueous mixture solution of ethanol and ammonia, and then water and ethanol for the subsequent metallation reactions to occur after phen grafting. Exposing the neutralized ITO-phen to 1:9 CH_2Cl_2/THF

solutions of the known compound[52] *cis*-[Ru(bpy)$_2$(CH$_3$CN)$_2$] (OTf)$_2$ (**1**, 5 mM, 50 °C, 2 h, bpy = 2,2'-bipyridine) resulted in displacement of the acetonitrile ligands to form the photoanode ITO-[(phen)Ru(bpy)$_2$](OTf)$_2$, with the Ru-polypyridyl chromophore covalently bonded at C5 to ITO. The solution of **1** could be reused several times for the metallation provided it was stored under N_2. The steps in the construction of the ITO-chromophore photoanode were investigated by cyclic voltammetry in a 0.1 M NBu_4PF_6 in CH_2Cl_2 electrolyte. Figure 2A and 2B show the CVs of the ITO-phen and bare ITO electrodes in this non-aqueous electrolyte. The CV of bare ITO is essentially featureless, while the CV of ITO-phen contains a broad oxidation response > 1.0 V versus Fc^+/Fc ($V_{Fc+/Fc}$), and broad reduction response < -1.0 $V_{Fc+/Fc}$. Figure 2C shows the CV of ITO-[(phen)Ru(bpy)$_2$]$^{2+}$ starting at -0.35 $V_{Fc+/Fc}$ with the first sweep in the positive direction. There was an oxidation peak at 0.95 $V_{Fc+/Fc}$ in the first anodic sweep that matches the reported $Ru^{2+/3+}$ oxidation potential.[59] The corresponding reduction peak was absent in the reverse sweep, showing that the Ru^{3+} complex was unstable under these conditions, and decomposed by an unknown process. There was a cathodic peak at -1.62 $V_{Fc+/Fc}$ that may have arisen from reduction of a phen-containing species remaining on ITO.[59] The estimated surface loading of the [(phen)Ru(bpy)$_2$]$^{2+}$ chromophore was 2.4×10^{-10} mol cm^{-2} based upon the charge under the $Ru^{2+/3+}$ anodic peak. This coverage matches the coverage of ITO by phen in ITO-phen (2.4×10^{-10} mol cm^{-2}, estimated from the charge for the 2e$^-$ reduction to 1,4-dihydropyridine-type compound). Further, the loading of Ru in ITO-[(phen)Ru(bpy)$_2$]$^{2+}$ was determined by dissolution into aqua regia and ICP-MS to be 2.3×10^{-10} mol cm^{-2}, quite consistent with the coverage obtained from cyclic voltammetry.

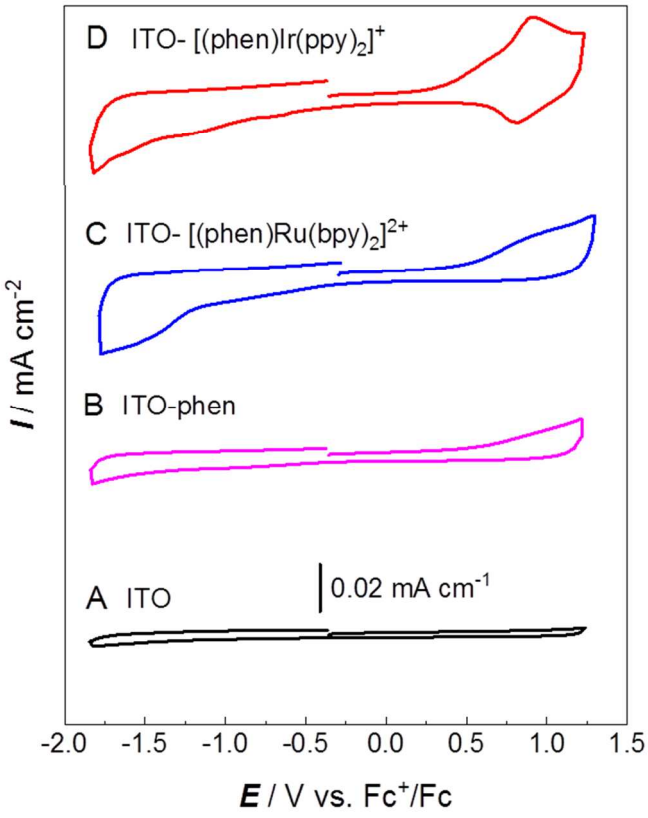

Figure 2. Cyclic voltammograms of the ITO electrodes throughout the chromophore grafting process in a N_2-saturated CH_2Cl_2 solution containing 0.1 M NBu_4PF_6, scan rate: 200 mV s^{-1}. (A) A bare ITO electrode, (B) an ITO-phen electrode, (C) an ITO-$[(phen)Ru(bpy)_2]^{2+}$ electrode, and (D) an ITO-$[(phen)Ir(ppy)_2]^{+}$ electrode.

The metallation can be repeated with the known compound[53] *cis*-$[Ir(ppy)_2(CH_3CN)_2]OTf$ (**2**, ppy = *ortho*-C_{phenyl} metallated 2-phenylpyridine) under the same conditions as for Ru. Figure 2D shows the cyclic voltammogram of the resulting ITO-$[(phen)Ir(ppy)_2]^{+}$ (0.1 M NBu_4PF_6, CH_2Cl_2) starting at -0.35 $V_{Fc+/Fc}$ and the first sweep in the positive direction. The $Ir^{3+/4+}$ redox couple peaks at 0.90 $V_{Fc+/Fc}$ and 0.81 $V_{Fc+/Fc}$ are similar to those reported for related Ir chromophores in the literature.[60] This redox couple is more reversible than the $Ru^{2+/3+}$ couple in ITO-$[(phen)Ru(bpy)_2]^{2+}$. The reduction peak in the first negative going sweep at -1.74 $V_{Fc+/Fc}$ may be

attributed to the irreversible reduction of the phenanthroline ligand on the photoelectrode.[60-61] The charge under the $Ir^{3+/4+}$ oxidation peak corresponds to a loading of Ir = 2.8×10^{-10} mol cm^{-2}. This loading agrees with the estimated coverage of phen in ITO-phen. Moreover, ICP-MS results after dissolution of Ir into aqua regia solution correspond to an Ir loading = 2.6×10^{-10} mol cm^{-2}, consistent with the Ir and phen coverages estimated with cyclic voltammetry. Taken together, the results from the Ru and Ir metallation show that this method is versatile and that little free phen ligand remains on the ITO surface after the metallation.

Figures 3A and 3B show the XPS spectra of the ITO-$[(phen)Ir(ppy)_2]^+$ and ITO-$[(phen)Ru(bpy)_2]^{2+}$ photoelectrodes, respectively. In Figure 3A, the XPS spectrum of ITO-$[(phen)Ir(ppy)_2]^+$ contains well-defined Ir 4f peaks. The Ir $4f_{7/2}$ peak at 62.8 eV is consistent with the Ir +3 oxidation state.[32] In Figure 3B, the XPS spectrum of the Ru $3d_{5/2}$ peak at 281.4 eV is consistent with the Ru +2.[47,62] The estimated atomic ratios of N:Ir and N:Ru from the XPS data are ~ 4:1 and 6:1, respectively, indicating that all the 1,10-phenanthroline groups are metallated, and that azo-coupling did not occur during the diazonium reduction.[63] Ir and Ru peaks were not observed in the XPS spectra of bare ITO or ITO-phen electrodes (Figure S12).

Figures 3C and 3D show the solid-state UV-vis absorption spectra of the ITO-$[(phen)Ir(ppy)_2]^+$ and ITO-$[(phen)Ru(bpy)_2]^{2+}$ photoelectrodes, respectively. The lower wavelength was set to 350 nm because ITO absorbs strongly below this value. The UV-vis absorption spectrum of ITO-$[(phen)Ir(ppy)_2]^+$ strongly resembles that of *cis*-$[Ir(ppy)_2(phen)]OTf$ in CH_2Cl_2 solution (Figure 3C, inset). The visible absorption spectrum results from overlapping metal-to-ligand charge transfer (^{1}MLCT, ^{3}MLCT) ($d\pi(Ir) \rightarrow \pi^*(phen)$), ligand-to-ligand charge transfer (^{1}LLCT, ^{3}LLCT), and ligand centered (LC) $^3\pi \rightarrow \pi^*$ transitions.[64] The mixing of the formally spin-forbidden ^{3}MLCT, ^{3}LLCT, and (^{3}LC) $^3\pi \rightarrow \pi^*$ with higher-lying ^{1}MLCT transitions allows for relatively intense

absorptions. This mixing arises from strong spin-orbit coupling induced by the heavy iridium(III) atom.[64-65]

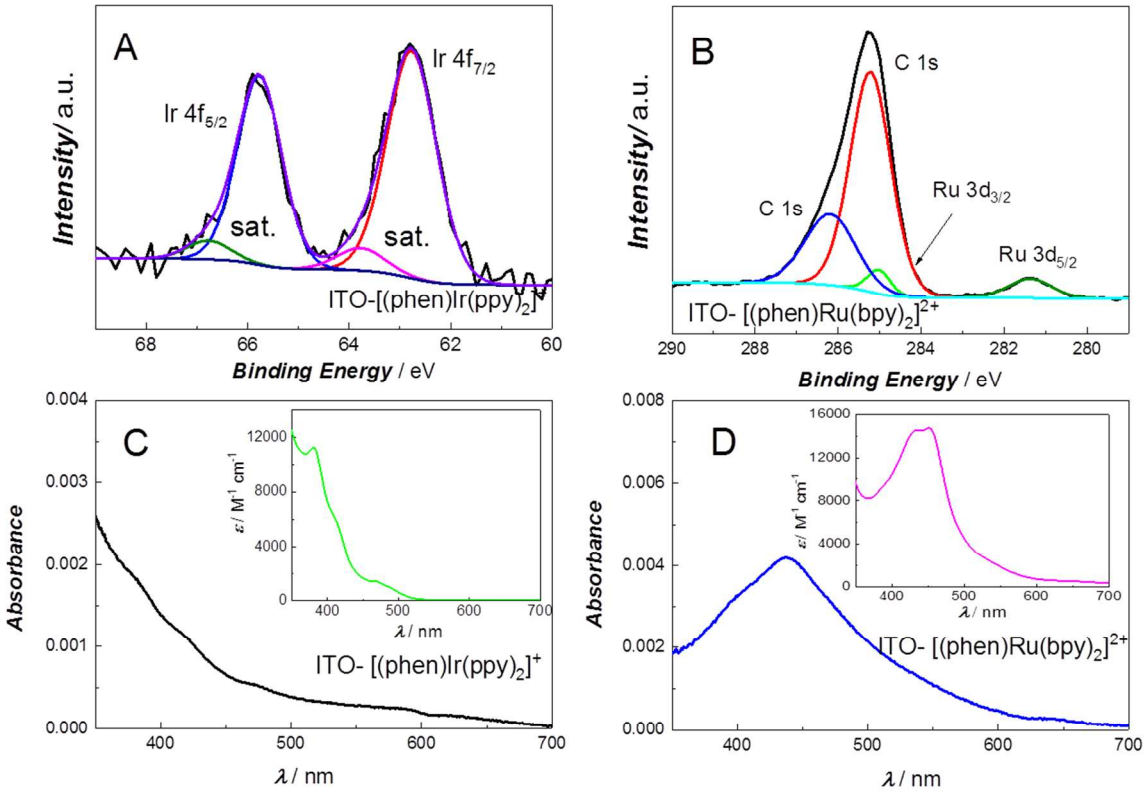

Figure 3. High resolution XPS spectra on (A) Ir 4f region of ITO-$[(phen)Ir(ppy)_2]^+$ electrode and (B) Ru 3d region of ITO-$[(phen)Ru(bpy)_2]^{2+}$ electrode. UV-vis absorption spectra of the (C) ITO-$[(phen)Ir(ppy)_2]^+$ and (D) ITO-$[(phen)Ru(bpy)_2]^{2+}$ electrodes with ITO absorbance deducted. The insets correspond to the UV-vis absorption spectra of the *cis*-$[Ir(ppy)_2(phen)]$ OTf and $[Ru(bpy)_2(phen)]$ $(OTf)_2$ in CH_2Cl_2 solution, respectively.

Figure 3D shows the solid-state UV-vis absorption spectrum of the ITO-$[(phen)Ru(bpy)_2]^{2+}$ photoelectrode. The absorption at 440 nm likely results from overlapping $d\pi(Ru)\rightarrow\pi(bpy)^*$ and $d\pi(Ru)\rightarrow\pi(phen)^*$ ^{1}MLCT absorptions.[66] The UV-vis spectrum of $[Ru(bpy)_2(phen)]^{2+}$ in CH_2Cl_2 solution contains a similar peak at 452 nm with a shoulder at 420 nm (Figure 3D, inset).[67]

The surface coverages (Γ) by Ir and Ru in ITO-$[(phen)Ir(ppy)_2]^+$ and ITO-$[(phen)Ru(bpy)_2]^{2+}$ were estimated from their solid-state UV-vis absorption spectra with equation 2, employing the molar extinction coefficients (ε) measured for *cis*-$[Ir(ppy)_2(phen)]^+$ and $[Ru(bpy)_2(phen)]^{2+}$ in CH_2Cl_2 solution at 440 nm.[2,68]

$$\Gamma(\text{moles per cm}^{-2}) = \frac{Absorbance}{\varepsilon(\text{M}^{-1}\text{cm}^{-1})} \quad (2)$$

The estimated coverages were 3.19×10^{-10} mol cm^{-2} ITO-$[(phen)Ir(ppy)_2]^+$, and 2.80×10^{-10} mol cm^{-2} in ITO-$[(phen)Ru(bpy)_2]^{2+}$. These values are comparable with those obtained from cyclic voltammetry and ICP-MS. Taken together, the results from cyclic voltammetry, ICP-MS, XPS, and UV-vis absorbance spectroscopy all show that most, if not all of the phen ligands in ITO-phen were converted into Ir- or Ru-chromophores by this procedure. It seems that the amount of 1,10-phenanthroline deposited on the surface limits the coverage of the chromophores. Further investigations of other grafting techniques may lead to higher loadings of chromophore.

High surface area TiO_2 (10 μm thick film) on FTO is readily converted into the photoelectrode TiO_2-$[(phen)Ru(bpy)_2]^{2+}$ utilizing the same procedure. The coverage by Ru in TiO_2-$[(phen)Ru(bpy)_2]^{2+}$ was 2.0×10^{-9} mol cm^{-2} as determined by cyclic voltammetry (Figure S7), UV-vis spectroscopy (Figure S13), and ICP-MS. For comparison, we prepared and adsorbed the common chromophore $[Ru(bpy)_2(4,4'\text{-}(PO_3H_2)_2bpy)]^{2+}$ onto the TiO_2/FTO using common methods reported in the literature.[54-55] The Ru coverage in this control photoanode (denoted as RuP-TiO_2) was ~ 4.5 times higher, 9.0×10^{-9} mol cm^{-2}, as measured by solid-state UV-vis absorption spectroscopy (Figure S14) and ICP-MS.

Figures 4 and 5 show the results of the photoelectrochemical activities and incident photon-to-current conversion efficiencies (IPCE) of the photoelectrodes in different solutions and pHs. Figure 4A shows the IPCE vs. wavelength plots of the photoanodes for photoelectrochemical

oxidation of 0.5 M triethylamine (Et_3N) in 0.1 M $NaClO_4$ solution (-0.3 V, pH = 12.6). Unlike TiO_2-$[(phen)Ru(bpy)_2]^{2+}$, the control RuP-TiO_2 bleached within 20 seconds of immersion into the basic solution. The IPCE for TiO_2-$[(phen)Ru(bpy)_2]^{2+}$ was 1.4% at 450 nm, 12 times higher than the bleached RuP-TiO_2 control. Figure 4B shows the long-term photoelectrochemical oxidation of triethylamine (2.3 mW cm^{-2}, 450 nm). TiO_2-$[(phen)Ru(bpy)_2]^{2+}$ was the most active. When the light was turned on at 300 s, a sharp increase in current is occurred, followed by a rapid decline over the first 400 s of illumination, then a more stable region. The initial photocurrent reached 8 μA cm^{-2}, a value 6 x that of TiO_2-phen, and 8 x TiO_2. The initial turnover frequency (TOF) was determined with eq 3 (i = photocurrent density, n = electron transfer number, Γ = surface coverage).[24,55]

$$\text{TOF } (h^{-1}) = \frac{3600\, i}{nF\Gamma} \qquad (3)$$

The initial TOF for TiO_2-$[(phen)Ru(bpy)_2]^{2+}$ was 74 h^{-1}, and dropped to 44 h^{-1} at 400 s illumination, during the initial decline. From 400 to 3000 s, the photocurrent only dropped by 7.6%. Figure 4C shows the photocurrent normalized to 200 s illumination time. The TiO_2-$[(phen)Ru(bpy)_2]^{2+}$ maintained 87% of photocurrent after 1000 s, and 81% after 3300 s.

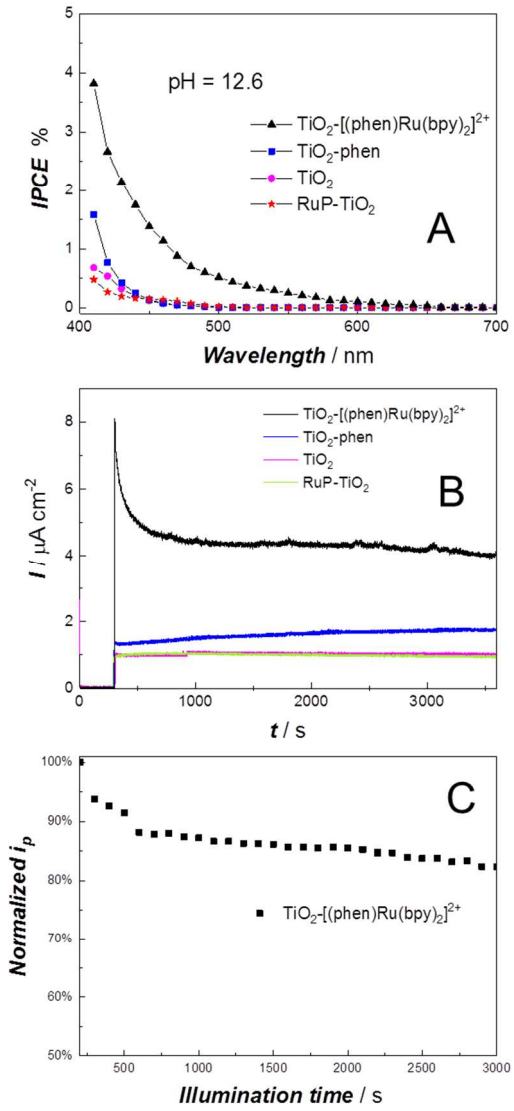

Figure 4. (A) The IPCE measurements and (B) Photoelectrochemical responses of the TiO_2-$[(phen)Ru(bpy)_2]^{2+}$, TiO_2-phen, bare TiO_2 and RuP-TiO_2 electrodes in 0.1 M $NaClO_4$ containing 0.5 M triethylamine at constant potential of -0.3 V under Ar (pH = 12.6); (C) Photocurrent normalized to current at 200 s illumination for TiO_2-$[(phen)Ru(bpy)_2]^{2+}$ electrode.

Figure 5A shows the IPCE vs. wavelength for the photooxidation of hydroquinone at neutral pH. The peak IPCE for the RuP-TiO_2 control was 6.3%, occurring at 450 nm. The IPCE for TiO_2-$[(phen)Ru(bpy)_2]^{2+}$ was 3.1% at 450 nm, and reached 5.5% at 410 nm. We note that the coverage by chromophore in the RuP-TiO_2 control was 4.5 times that of TiO_2-

$[(phen)Ru(bpy)_2]^{2+}$ (*vide supra*). Figure 5B shows the long-term stability results for photooxidation of hydroquinone. An immediate increase of current occurs upon exposure of all electrodes to light. The photocurrent was more stable for all the electrodes under neutral conditions than they were in base, and the large initial drop-off was absent. The initial photocurrent for TiO_2-$[(phen)Ru(bpy)_2]^{2+}$ was 25 μA cm^{-2}, corresponding to TOF = 231 h^{-1}, and the photocurrent increased slightly during the first 200 s illumination, then slowly decreased to 22 μA cm^{-2} at 3300 s illumination. The initial photocurrent for RuP-TiO_2 was 45 μA cm^{-2}, corresponding to TOF = 92 h^{-1}, but the photocurrent dropped to 34 μA cm^{-2} at 3300 s illumination.

Figure 5C compares the photocurrent for TiO_2-$[(phen)Ru(bpy)_2]^{2+}$ and RuP-TiO_2 normalized to Ru surface coverage (2.0×10^{-9} mol cm^{-2} for TiO_2-$[(phen)Ru(bpy)_2]^{2+}$, and 9.0×10^{-9} mol cm^{-2} for RuP-TiO_2). The normalized photocurrent for TiO_2-$[(phen)Ru(bpy)_2]^{2+}$ was ~ 3 x that of RuP-TiO_2 throughout the process. The origin of this enhanced normalized photocurrent is under investigation. Figure 5D compares the stability of the TiO_2-$[(phen)Ru(bpy)_2]^{2+}$ and RuP-TiO_2 electrodes by normalizing activities to the current at 200 s of illumination. The TiO_2-$[(phen)Ru(bpy)_2]^{2+}$ maintained 97% of photocurrent after 1000 s, and 85% after 3300 s. The control RuP-TiO_2 dropped to 88% after 1000 s, and down to 69% after 3300 s. ICP-MS showed that 33% of the surface Ru was lost to the solution over 3300 s for the control RuP-TiO_2, compared to 10% for TiO_2-$[(phen)Ru(bpy)_2]^{2+}$.

The TiO_2-$[(phen)Ir(ppy)_2]^{+}$ electrodes were also prepared using this method. The coverage of Ir on the TiO_2-$[(phen)Ir(ppy)_2]^{+}$ is 2.2×10^{-9} mol cm^{-2} as determined by cyclic voltammetry (Figure S7), UV-vis spectroscopy (Figure S13) and ICP-MS. Figure 6A shows the IPCE results of the TiO_2-$[(phen)Ir(ppy)_2]^{+}$ and TiO_2-phen in neutral (hydroquinone) and basic (Et_3N)

electrolytes. Under neutral conditions, the peak IPCE for TiO_2-$[(phen)Ir(ppy)_2]^+$ reached 4.0% at 410 nm, and decreased with increasing wavelength. Under alkaline conditions, the peak IPCE value reached 2.0% at 410 nm. Compared with the IPCE of TiO_2-phen, the TiO_2-$[(phen)Ir(ppy)_2]^+$ does not lead to a substantial IPCE enhancement possibly due to its less favorable light harvesting in the visible region.

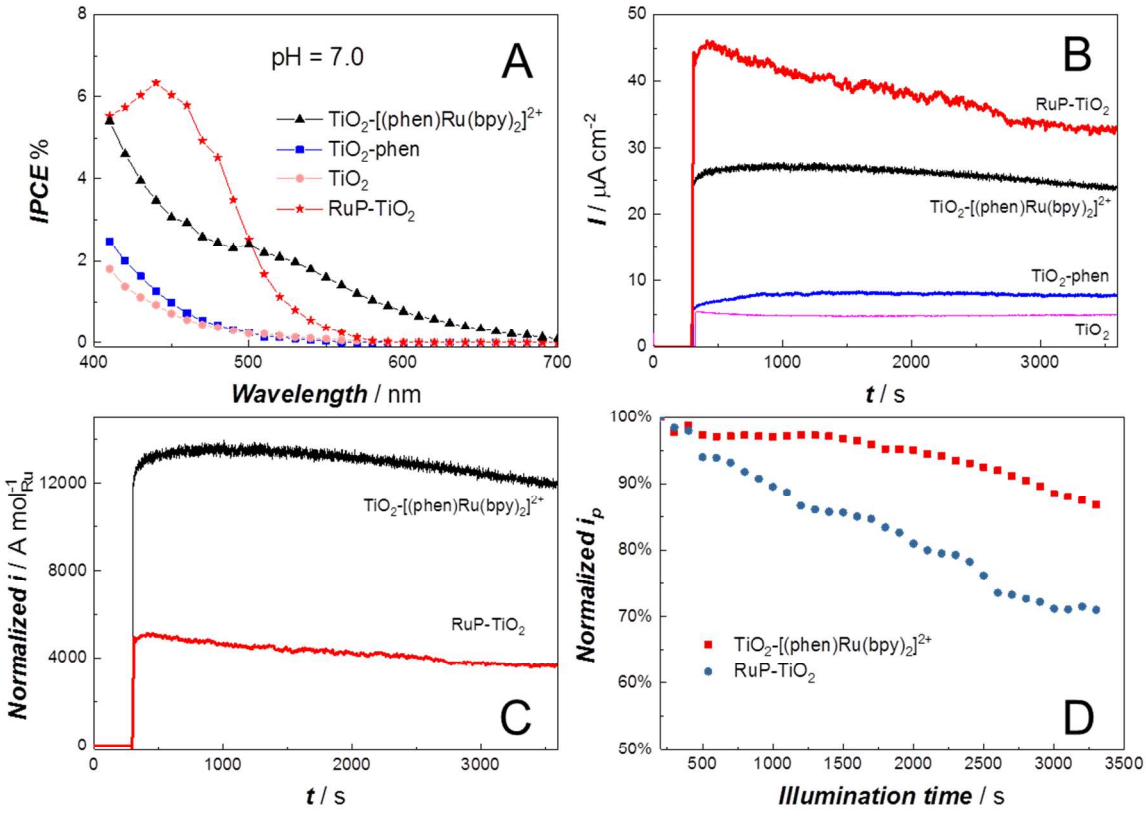

Figure 5. (A) The IPCE measurements and (B) Photoelectrochemical responses of TiO_2-$[(phen)Ru(bpy)_2]^{2+}$, TiO_2-phen, bare TiO_2 and RuP-TiO_2 electrodes in 0.1 M $NaClO_4$ with 0.02 M hydroquinone under Ar at 0 V; (C) Photocurrent response normalized to moles of surface Ru for TiO_2-$[(phen)Ru(bpy)_2]^{2+}$ and RuP-TiO_2 electrodes in 0.1 M $NaClO_4$ with 0.02 M hydroquinone under Ar at 0 V; (D) Photocurrent stability comparison between TiO_2-$[(phen)Ru(bpy)_2]^{2+}$ and RuP-TiO_2 normalized to the 200 s illumination current for each electrode. All solutions are stirred at 500 rpm.

Figure 6B shows the long-term photocurrent responses of TiO_2-$[(phen)Ir(ppy)_2]^+$ electrode under neutral (0.1 M $NaClO_4$ containing 0.02 M hydroquinone) and basic (0.1 M $NaClO_4$ containing 0.5 M Et_3N) conditions under 450 nm 2.3 mW cm^{-2} irradiation. In neutral solution, the initial photocurrent for TiO_2-$[(phen)Ir(ppy)_2]^+$ reached 22 μA cm^{-2}, corresponding to TOF = 187 h^{-1}. The TiO_2-$[(phen)Ir(ppy)_2]^+$ electrode maintained 74% photocurrent after 3300 s illumination relative to the photocurrent at 200 s. In basic solution, the electrode reached 8 μA cm^{-2} (TOF = 68 h^{-1}) initially, then dropped quickly. Only 40% photocurrent was maintained after 3300 s relative to that of 200 s illumination. Compared with TiO_2-$[(phen)Ru(bpy)_2]^{2+}$, TiO_2-$[(phen)Ir(ppy)_2]^+$ electrode showed inferior stability in both neutral and basic conditions.

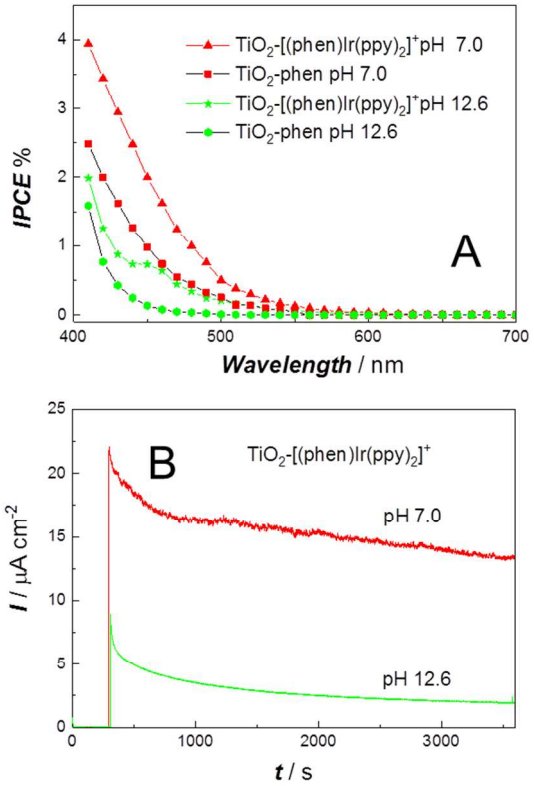

Figure 6. (A) The IPCE measurements and (B) Photoelectrochemical responses of the TiO_2-$[(phen)Ir(ppy)_2]^+$ and TiO_2-phen electrodes in 0.1 M $NaClO_4$ containing 0.5 M triethylamine (pH

= 12.6) at constant potential of -0.3 V, and in 0.1 M $NaClO_4$ with 0.02 M hydroquinone (pH = 7.0) at 0 V under Ar. All the solutions are stirred at 500 rpm.

The IPCE of all the photoelectrodes were higher under neutral conditions than they were in base. Similar results were observed by Meyer et al., who attributed the higher IPCE to a decrease in the rate of back electron transfer as the pH is decreased.[55] Other factors like the difference in the redox potentials of hydroquinone and triethylamine could also affect the electron transfer kinetics. More investigation is required to determine the origins of this phenomenon.

CONCLUSIONS

We have demonstrated a versatile, two-step process to prepare semiconductors-chromophore assembly. We prepared demonstration photoelectrodes with Ru and Ir chromophores anchored to ITO or TiO_2 surfaces by covalent bond. The strong linkage between the chromophores and the TiO_2 surface is more stable under neutral and alkaline conditions than that with phosphonate ester bridges, and the sensitized electrodes can potentially be paired with a suitable catalyst and be used for photoelectrochemical oxidation of water in a wide pH range. Further studies to extend the method to other systems to construct water oxidation and CO_2 reduction photoelectrodes are under way in our laboratories.

ASSOCIATED CONTENT

Supporting Information. The following files are available free of charge.

NMR of synthesized complexes; Electrochemical studies carried out on photoanodes; XPS, UV-vis and ToF-SIMS characterizations.

AUTHOR INFORMATION

Corresponding Author

* Email: sbergens@ualberta.ca

Author Contributions

The manuscript was written through contributions of all authors. All authors have given approval to the final version of the manuscript.

Funding Sources

Canada First Research Excellence Fund (CFREF)

Future Energy Systems Research Initiative (FESRI)

Natural Sciences and Engineering Research Council of Canada (NSERC)

University of Alberta

Notes

The authors declare no competing financial interests.

ACKNOWLEDGMENT

Authors thank Canada First Research Excellence Fund (CFREF), Future Energy Systems Research Initiative (FESRI), Natural Sciences and Engineering Research Council of Canada (NSERC), Alberta Ingenuity: Technology Futures, and the University of Alberta for supporting this work. Authors thank Guangcheng Chen for ICP-MS measurements and Anqiang He for XPS measurements.

REFERENCES

(1) Lewis, N. S. Research Opportunities to Advance Solar Energy Utilization. *Science* **2016,** *351*, 353.

(2) O'Regan, B.; Gratzel, M. A Low-Cost, High-Efficiency Solar Cell Based on Dye-Sensitized Colloidal TiO_2 Films. *Nature* **1991,** *353*, 737-740.

(3) Grätzel, M. Photoelectrochemical Cells. *Nature* **2001,** *414*, 338-344.

(4) Yu, Z.; Li, F.; Sun, L. Recent Advances in Dye-Sensitized Photoelectrochemical Cells for Solar Hydrogen Production Based on Molecular Components. *Energy Environ. Sci.* **2015,** *8*, 760-775.

(5) Walter, M. G.; Warren, E. L.; McKone, J. R.; Boettcher, S. W.; Mi, Q.; Santori, E. A.; Lewis, N. S. Solar Water Splitting Cells. *Chem. Rev.* **2010,** *110*, 6446-6473.

(6) Fujishima, A.; Honda, K. Electrochemical Photolysis of Water at a Semiconductor Electrode. *Nature* **1972,** *238*, 37-38.

(7) Schultz, D. M.; Yoon, T. P. Solar Synthesis: Prospects in Visible Light Photocatalysis. *Science* **2014,** *343*, 985.

(8) Moniz, S. J. A.; Shevlin, S. A.; Martin, D. J.; Guo, Z.-X.; Tang, J. Visible-Light Driven Heterojunction Photocatalysts for Water Splitting - a Critical Review. *Energy Environ. Sci.* **2015,** *8*, 731-759.

(9) Hisatomi, T.; Kubota, J.; Domen, K. Recent Advances in Semiconductors for Photocatalytic and Photoelectrochemical Water Splitting. *Chem. Soc. Rev.* **2014,** *43*, 7520-7535.

(10) Higashi, T.; Kaneko, H.; Minegishi, T.; Kobayashi, H.; Zhong, M.; Kuang, Y.; Hisatomi, T.; Katayama, M.; Takata, T.; Nishiyama, H.; Yamada, T.; Domen, K. Overall Water Splitting by Photoelectrochemical Cells Consisting of $(ZnSe)_{0.85}(CuIn_{0.7}Ga_{0.3}Se_2)_{0.15}$ Photocathodes and $BiVO_4$ Photoanodes. *Chem. Commun.* **2017,** *53*, 11674-11677.

(11) Liu, X.; Wang, F.; Wang, Q. Nanostructure-Based WO_3 Photoanodes for Photoelectrochemical Water Splitting. *Phys. Chem. Chem. Phys.* **2012,** *14*, 7894-7911.

(12) Wang, S.; Chen, P.; Yun, J. H.; Hu, Y.; Wang, L. An Electrochemically Treated $BiVO_4$ Photoanode for Efficient Photoelectrochemical Water Splitting. *Angew. Chem.* **2017,** *129*, 8620-8624.

(13) Wang, Q.; Hisatomi, T.; Jia, Q.; Tokudome, H.; Zhong, M.; Wang, C.; Pan, Z.; Takata, T.; Nakabayashi, M.; Shibata, N.; Li, Y.; Sharp, I. D.; Kudo, A.; Yamada, T.; Domen, K. Scalable Water Splitting on Particulate Photocatalyst Sheets with a Solar-to-Hydrogen Energy Conversion Efficiency Exceeding 1%. *Nat. Mater.* **2016,** *15*, 611-615.

(14) Call, R. W.; Alibabaei, L.; Dillon, R. J.; Knauf, R. R.; Nayak, A.; Dempsey, J. L.; Papanikolas, J. M.; Lopez, R. Growth and Post-Deposition Treatments of $SrTiO_3$ Films for Dye-Sensitized Photoelectrosynthesis Cell Applications. *ACS Appl. Mater. Interfaces* **2016,** *8*, 12282-12290.

(15) Asahi, R.; Morikawa, T.; Ohwaki, T.; Aoki, K.; Taga, Y. Visible-Light Photocatalysis in Nitrogen-Doped Titanium Oxides. *Science* **2001,** *293*, 269-271.

(16) Brennaman, M. K.; Dillon, R. J.; Alibabaei, L.; Gish, M. K.; Dares, C. J.; Ashford, D. L.; House, R. L.; Meyer, G. J.; Papanikolas, J. M.; Meyer, T. J. Finding the Way to Solar Fuels with Dye-Sensitized Photoelectrosynthesis Cells. *J. Am. Chem. Soc.* **2016,** *138*, 13085-13102.

(17) Xu, P.; McCool, N. S.; Mallouk, T. E. Water Splitting Dye-Sensitized Solar Cells. *Nano Today* **2017,** *14*, 42-58.

(18) Dillon, R. J.; Alibabaei, L.; Meyer, T. J.; Papanikolas, J. M. Enabling Efficient Creation of Long-Lived Charge-Separation on Dye-Sensitized NiO Photocathodes. *ACS Appl. Mater. Interfaces* **2017,** *9*, 26786-26796.

(19) Evans, R. C.; Douglas, P.; Winscom, C. J. Coordination Complexes Exhibiting Room-Temperature Phosphorescence: Evaluation of Their Suitability as Triplet Emitters in Organic Light Emitting Diodes. *Coord. Chem. Rev.* **2006,** *250*, 2093-2126.

(20) Caspar, J. V.; Meyer, T. J. Photochemistry of MLCT Excited States. Effect of Nonchromophoric Ligand Variations on Photophysical Properties in the Series cis-$Ru(bpy)_2L_2^{2+}$. *Inorg. Chem.* **1983,** *22*, 2444-2453.

(21) Burian, M.; Syrgiannis, Z.; La Ganga, G.; Puntoriero, F.; Natali, M.; Scandola, F.; Campagna, S.; Prato, M.; Bonchio, M.; Amenitsch, H.; Sartorel, A. Ruthenium Based Photosensitizer/Catalyst Supramolecular Architectures in Light Driven Water Oxidation. *Inorg. Chim. Acta* **2017,** *454*, 171-175.

(22) Jiang, J.; Sherman, B. D.; Zhao, Y.; He, R.; Ghiviriga, I.; Alibabaei, L.; Meyer, T. J.; Leem, G.; Schanze, K. S. Polymer Chromophore-Catalyst Assembly for Solar Fuel Generation. *ACS Appl. Mater. Interfaces* **2017,** *9*, 19529-19534.

(23) Youngblood, W. J.; Lee, S.-H. A.; Kobayashi, Y.; Hernandez-Pagan, E. A.; Hoertz, P. G.; Moore, T. A.; Moore, A. L.; Gust, D.; Mallouk, T. E. Photoassisted Overall Water Splitting in a Visible Light-Absorbing Dye-Sensitized Photoelectrochemical Cell. *J. Am. Chem. Soc.* **2009,** *131*, 926-927.

(24) Gao, Y.; Ding, X.; Liu, J.; Wang, L.; Lu, Z.; Li, L.; Sun, L. Visible Light Driven Water Splitting in a Molecular Device with Unprecedentedly High Photocurrent Density. *J. Am. Chem. Soc.* **2013,** *135*, 4219-4222.

(25) Sherman, B. D.; Xie, Y.; Sheridan, M. V.; Wang, D.; Shaffer, D. W.; Meyer, T. J.; Concepcion, J. J. Light-Driven Water Splitting by a Covalently Linked Ruthenium-Based Chromophore–Catalyst Assembly. *ACS Energy Lett.* **2017,** *2*, 124-128.

(26) Ashford, D. L.; Gish, M. K.; Vannucci, A. K.; Brennaman, M. K.; Templeton, J. L.; Papanikolas, J. M.; Meyer, T. J. Molecular Chromophore–Catalyst Assemblies for Solar Fuel Applications. *Chem. Rev.* **2015,** *115*, 13006-13049.

(27) Liu, X.; Yao, B.; Zhang, Z.; Zhao, X.; Zhang, B.; Wong, W. Y.; Cheng, Y.; Xie, Z. Power-Efficient Solution-Processed Red Organic Light-Emitting Diodes Based on an Exciplex Host and a Novel Phosphorescent Iridium Complex. *J. Mater. Chem. C* **2016,** *4*, 5787-5794.

(28) Clemente-León, M.; Coronado, E.; López-Muñoz, Á.; Repetto, D.; Ito, T.; Konya, T.; Yamase, T.; Constable, E. C.; Housecroft, C. E.; Doyle, K.; Graber, S. Dual-Emissive Photoluminescent Langmuir−Blodgett Films of Decatungstoeuropate and an Amphiphilic Iridium Complex. *Langmuir* **2010,** *26*, 1316-1324.

(29) Joya, K. S.; Subbaiyan, N. K.; D'Souza, F.; de Groot, H. J. M. Surface-Immobilized Single-Site Iridium Complexes for Electrocatalytic Water Splitting. *Angew. Chem. Int. Ed.* **2012,** *51*, 9601-9605.

(30) Piper, D. J. E.; Barbante, G. J.; Brack, N.; Pigram, P. J.; Hogan, C. F. Highly Stable ECL Active Films Formed by the Electrografting of a Diazotized Ruthenium Complex Generated in Situ from the Amine. *Langmuir* **2011,** *27*, 474-480.

(31) Nguyen, V. Q.; Sun, X.; Lafolet, F.; Audibert, J.-F.; Miomandre, F.; Lemercier, G.; Loiseau, F.; Lacroix, J.-C. Unprecedented Self-Organized Monolayer of a Ru(II) Complex by Diazonium Electroreduction. *J. Am. Chem. Soc.* **2016,** *138*, 9381-9384.

(32) deKrafft, K. E.; Wang, C.; Xie, Z.; Su, X.; Hinds, B. J.; Lin, W. Electrochemical Water Oxidation with Carbon-Grafted Iridium Complexes. *ACS Appl. Mater. Interfaces* **2012,** *4*, 608-613.

(33) Pho, T. V.; Sheridan, M. V.; Morseth, Z. A.; Sherman, B. D.; Meyer, T. J.; Papanikolas, J. M.; Schanze, K. S.; Reynolds, J. R. Efficient Light-Driven Oxidation of Alcohols Using an Organic Chromophore–Catalyst Assembly Anchored to TiO_2. *ACS Appl. Mater. Interfaces* **2016,** *8*, 9125-9133.

(34) Takijiri, K.; Morita, K.; Nakazono, T.; Sakai, K.; Ozawa, H. Highly Stable Chemisorption of Dyes with Pyridyl Anchors over TiO_2: Application in Dye-Sensitized Photoelectrochemical Water Reduction in Aqueous Media. *Chem. Commun.* **2017,** *53*, 3042-3045.

(35) Hanson, K.; Brennaman, M. K.; Luo, H.; Glasson, C. R. K.; Concepcion, J. J.; Song, W.; Meyer, T. J. Photostability of Phosphonate-Derivatized, Ru^{II} Polypyridyl Complexes on Metal Oxide Surfaces. *ACS Appl. Mater. Interfaces* **2012,** *4*, 1462-1469.

(36) Hyde, J. T.; Hanson, K.; Vannucci, A. K.; Lapides, A. M.; Alibabaei, L.; Norris, M. R.; Meyer, T. J.; Harrison, D. P. Electrochemical Instability of Phosphonate-Derivatized, Ruthenium(III) Polypyridyl Complexes on Metal Oxide Surfaces. *ACS Appl. Mater. Interfaces* **2015,** *7*, 9554-9562.

(37) Alibabaei, L.; Dillon, R. J.; Reilly, C. E.; Brennaman, M. K.; Wee, K.-R.; Marquard, S. L.; Papanikolas, J. M.; Meyer, T. J. Chromophore-Catalyst Assembly for Water Oxidation Prepared by Atomic Layer Deposition. *ACS Appl. Mater. Interfaces* **2017,** *9*, 39018-39026.

(38) Wee, K.-R.; Brennaman, M. K.; Alibabaei, L.; Farnum, B. H.; Sherman, B.; Lapides, A. M.; Meyer, T. J. Stabilization of Ruthenium(II) Polypyridyl Chromophores on Nanoparticle Metal-Oxide Electrodes in Water by Hydrophobic PMMA Overlayers. *J. Am. Chem. Soc.* **2014,** *136*, 13514-13517.

(39) Brennan, B. J.; Llansola Portoles, M. J.; Liddell, P. A.; Moore, T. A.; Moore, A. L.; Gust, D. Comparison of Silatrane, Phosphonic Acid, and Carboxylic Acid Functional Groups for Attachment of Porphyrin Sensitizers to TiO_2 in Photoelectrochemical Cells. *Phys. Chem. Chem. Phys.* **2013,** *15*, 16605-16614.

(40) Materna, K. L.; Rudshteyn, B.; Brennan, B. J.; Kane, M. H.; Bloomfield, A. J.; Huang, D. L.; Shopov, D. Y.; Batista, V. S.; Crabtree, R. H.; Brudvig, G. W. Heterogenized Iridium Water-Oxidation Catalyst from a Silatrane Precursor. *ACS Catal.* **2016,** *6*, 5371-5377.

(41) Brennan, B. J.; Koenigsmann, C.; Materna, K. L.; Kim, P. M.; Koepf, M.; Crabtree, R. H.; Schmuttenmaer, C. A.; Brudvig, G. W. Surface-Induced Deprotection of THP-Protected Hydroxamic Acids on Titanium Dioxide. *J. Phys. Chem. C* **2016,** *120*, 12495-12502.

(42) Surendranath, Y.; Kanan, M. W.; Nocera, D. G. Mechanistic Studies of the Oxygen Evolution Reaction by a Cobalt-Phosphate Catalyst at Neutral pH. *J. Am. Chem. Soc.* **2010,** *132*, 16501-16509.

(43) Watanabe, M.; Motoo, S. Electrocatalysis by Adatoms: Part III. Enhancement of the Oxidation of Carbon Monoxide on Platinum by Ruthenium Adatoms. *J. Electroanal. Chem. Interfacial Electrochem.* **1975,** *60*, 275-283.

(44) Belanger, D.; Pinson, J. Electrografting: a Powerful Method for Surface Modification. *Chem. Soc. Rev.* **2011,** *40*, 3995-4048.

(45) Chung, D. J.; Oh, S. H.; Komathi, S.; Gopalan, A. I.; Lee, K. P.; Choi, S. H. One-Step Modification of Various Electrode Surfaces Using Diazonium Salt Compounds and the Application of This Technology to Electrochemical DNA (E-DNA) Sensors. *Electrochim. Acta* **2012,** *76*, 394-403.

(46) Lund, T.; Nguyen, P. T.; Ruhland, T. Electrochemical Grafting of TiO_2-Based Photao-Anodes and Its Effect in Dye-Sensitized Solar Cells. *J. Electroanal. Chem.* **2015,** *758*, 85-92.

(47) Agnes, C.; Arnault, J.-C.; Omnes, F.; Jousselme, B.; Billon, M.; Bidan, G.; Mailley, P. XPS Study of Ruthenium Tris-Bipyridine Electrografted from Diazonium Salt Derivative on Microcrystalline Boron Doped Diamond. *Phys. Chem. Chem. Phys.* **2009,** *11*, 11647-11654.

(48) Bangle, R.; Sampaio, R. N.; Troian-Gautier, L.; Meyer, G. J. Surface Grafting of Ru(II) Diazonium-Based Sensitizers on Metal Oxides Enhances Alkaline Stability for Solar Energy Conversion. *ACS Appl. Mater. Interfaces* **2018,** *10*, 3121-3132.

(49) Dragonetti, C.; Valore, A.; Colombo, A.; Righetto, S.; Trifiletti, V. Simple Novel Cyclometallated Iridium Complexes for Potential Application in Dye-Sensitized Solar Cells. *Inorg. Chim. Acta* **2012,** *388*, 163-167.

(50) Xu, S.; Zhou, C.; Yang, Y.; Hu, H.; Sebo, B.; Chen, B.; Tai, Q.; Zhao, X. Effects of Ethanol on Optimizing Porous Films of Dye-Sensitized Solar Cells. *Energy Fuels* **2011,** *25*, 1168-1172.

(51) Shul, G.; Weissmann, M.; Bélanger, D. Electrochemical Characterization of Glassy Carbon Electrode Modified with 1,10-Phenanthroline Groups by Two Pathways: Reduction of the Corresponding Diazonium Ions and Reduction of Phenanthroline. *Electrochim. Acta* **2015,** *162*, 146-155.

(52) Liu, Y.; Turner, D. B.; Singh, T. N.; Angeles-Boza, A. M.; Chouai, A.; Dunbar, K. R.; Turro, C. Ultrafast Ligand Exchange: Detection of a Pentacoordinate Ru(II) Intermediate and Product Formation. *J. Am. Chem. Soc.* **2009,** *131*, 26-27.

(53) Schmid, B.; Garces, F. O.; Watts, R. J. Synthesis and Characterizations of Cyclometalated Iridium(III) Solvento Complexes. *Inorg. Chem.* **1994,** *33*, 9-14.

(54) Gillaizeau-Gauthier, I.; Odobel, F.; Alebbi, M.; Argazzi, R.; Costa, E.; Bignozzi, C. A.; Qu, P.; Meyer, G. J. Phosphonate-Based Bipyridine Dyes for Stable Photovoltaic Devices. *Inorg. Chem.* **2001,** *40*, 6073-6079.

(55) Brennaman, M. K.; Patrocinio, A. O. T.; Song, W.; Jurss, J. W.; Concepcion, J. J.; Hoertz, P. G.; Traub, M. C.; Murakami Iha, N. Y.; Meyer, T. J. Interfacial Electron Transfer Dynamics Following Laser Flash Photolysis of $[Ru(bpy)_2((4,4' - PO_3H_2)_2bpy)]^{2+}$ in TiO_2 Nanoparticle Films in Aqueous Environments. *ChemSusChem* **2011,** *4*, 216-227.

(56) Yeşildağ, A.; Ekinci, D. Covalent Attachment of Pyridine-Type Molecules to Glassy Carbon Surfaces by Electrochemical Reduction of in Situ Generated Diazonium Salts. Formation of Ruthenium Complexes on Ligand-Modified Surfaces. *Electrochim. Acta* **2010,** *55*, 7000-7009.

(57) Shi, W.; Wu, K.-H.; Xu, J.; Zhang, Q.; Zhang, B.; Su, D. S. Enhanced Stability of Immobilized Platinum Nanoparticles through Nitrogen Heteroatoms on Doped Carbon Supports. *Chem. Mater.* **2017,** *29*, 8670-8678.

(58) Shul, G.; Weissmann, M.; Bélanger, D. Electrochemical Formation of an Ultrathin Electroactive Film from 1,10-Phenanthroline on a Glassy Carbon Electrode in Acidic Electrolyte. *Langmuir* **2014,** *30*, 6612-6621.

(59) Caspar, J. V.; Meyer, T. J. hotochemistry of MLCT Excited States. Effect of Nonchromophoric Ligand Variations on Photophysical Properties in the Series cis-$Ru(bpy)_2L_2^{2+}$. *Inorg. Chem.* **1983,** *22*, 2444-2453.

(60) Dragonetti, C.; Falciola, L.; Mussini, P.; Righetto, S.; Roberto, D.; Ugo, R.; Valore, A.; De Angelis, F.; Fantacci, S.; Sgamellotti, A.; Ramon, M.; Muccini, M. The Role of Substituents on Functionalized 1,10-Phenanthroline in Controlling the Emission Properties of Cationic Iridium(III) Complexes of Interest for Electroluminescent Devices. *Inorg. Chem.* **2007,** *46*, 8533-8547.

(61) Kim, J. I.; Shin, I.; Kim, H.; Lee, J. Efficient Electrogenerated Chemiluminescence from Cyclometalated Iridium(III) Complexes. *J. Am. Chem. Soc.* **2005,** *127*, 1614-1615.

(62) Liu, G.; Klein, A.; Thissen, A.; Jaegermann, W. Electronic Properties and Interface Characterization of Phthalocyanine and Ru-Polypyridine Dyes on TiO_2 Surface. *Surf. Sci.* **2003,** *539*, 37-48.

(63) Lund, T.; Nguyen, P. T.; Ruhland, T. Electrochemical Grafting of TiO_2-Based Photo-Anodes and Its Effect in Dye-Sensitized Solar Cells. *J. Electroanal. Chem.* **2015,** *758*, 85-92.

(64) Tang, H.; Li, Y.; Chen, Q.; Chen, B.; Qiao, Q.; Yang, W.; Wu, H.; Cao, Y. Efficient Yellow–Green Light-Emitting Cationic Iridium Complexes Based on 1,10-Phenanthroline Derivatives Containing Oxadiazole-Triphenylamine Unit. *Dyes Pigm.* **2014,** *100*, 79-86.

(65) Yang, H.; Meng, G.; Zhou, Y.; Tang, H.; Zhao, J.; Wang, Z. The Photoluminescent Properties of New Cationic Iridium(III) Complexes Using Different Anions and Their Applications in White Light-Emitting Diodes. *Materials* **2015,** *8*, 5296.

(66) Ji, S.; Wu, W.; Wu, W.; Song, P.; Han, K.; Wang, Z.; Liu, S.; Guo, H.; Zhao, J. Tuning the Luminescence Lifetimes of Ruthenium(II) Polypyridine Complexes and Its Application in Luminescent Oxygen Sensing. *J. Mater. Chem.* **2010,** *20*, 1953-1963.

(67) Felcmann, C.; Alt, R.; Greiner, G.; Rau, H.; Worner, M. Chiral Modified Electrodes. Part 1. Preparation and Characterization of a Polymeric $[Ru(4\text{-methyl-}4'\text{-vinylbipyridine})_3]^{2+}$ Electrode. *Phys. Chem. Chem. Phys.* **2000,** *2*, 3483-3489.

(68) Sabuzi, F.; Tiravia, M.; Vecchi, A.; Gatto, E.; Venanzi, M.; Floris, B.; Conte, V.; Galloni, P. Deposition of Tetraferrocenylporphyrins on ITO Surfaces for Photo-Catalytic O_2 Activation. *Dalton Trans.* **2016,** *45*, 14745-14753.

TOC

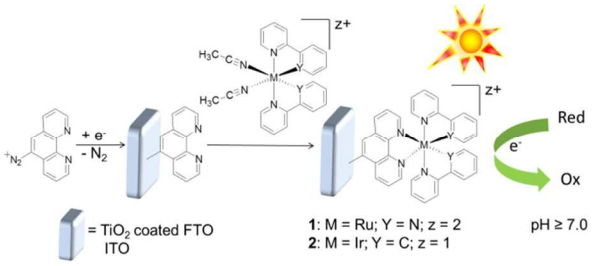

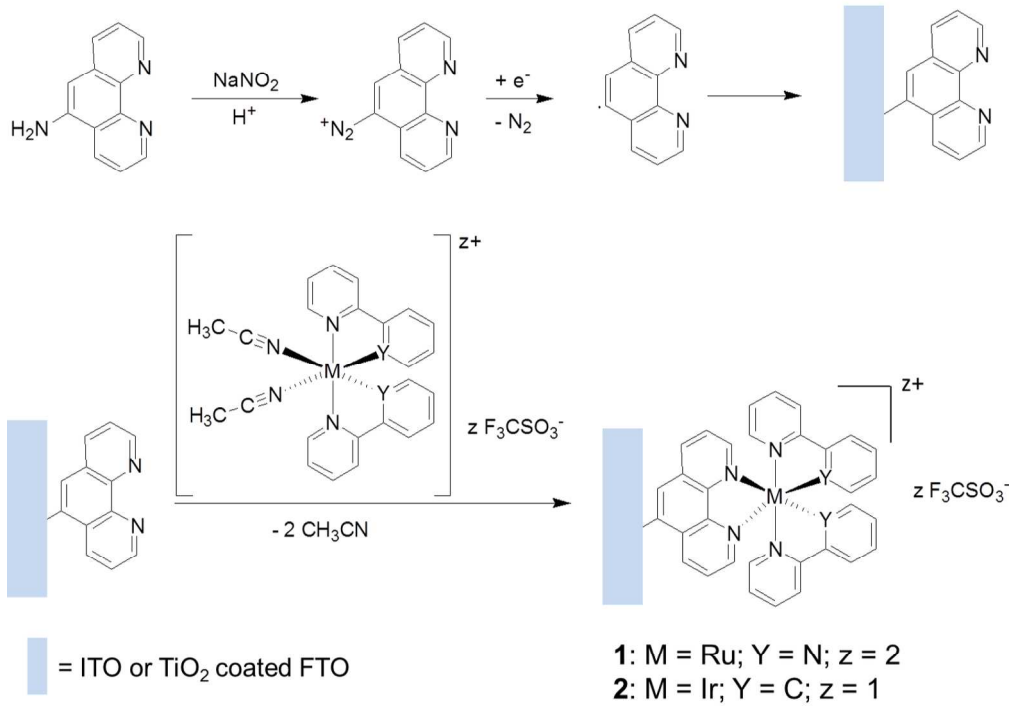

Scheme 1. Illustration of the electrochemical deposition of 5-diazo-1,10-phenanthroline cation, and subsequent formation of semiconductor-chromophore electrode.

215x166mm (300 x 300 DPI)

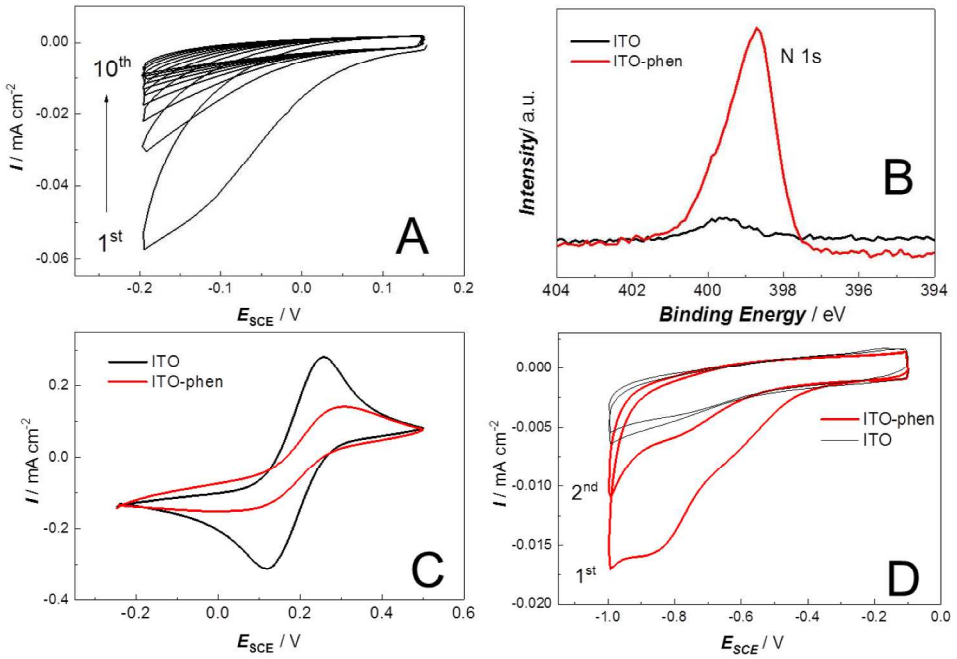

Figure 1. (A) Cyclic voltammogram of the ITO electrode in a 0.1 M H2SO4 solution containing 5-amino-1,10-phenanthroline (1 mM) and NaNO2 (2 mM), scan rate 50 mV s-1; (B) High resolution N 1s region XPS spectra of the ITO electrode before and after 1,10-phenanthroline deposition; (C) Cyclic voltammograms for the bare ITO and 1,10-phenanthroline modified ITO electrode in 0.1 M KCl solution containing 5 mM Fe(CN)63- at scan rate of 20 mV s-1; (D) Cyclic voltammograms of the ITO-phen and bare ITO electrodes in a N2-saturated 0.1 M Na2SO4 solution and a scan rate of 50 mV s-1.

297x210mm (300 x 300 DPI)

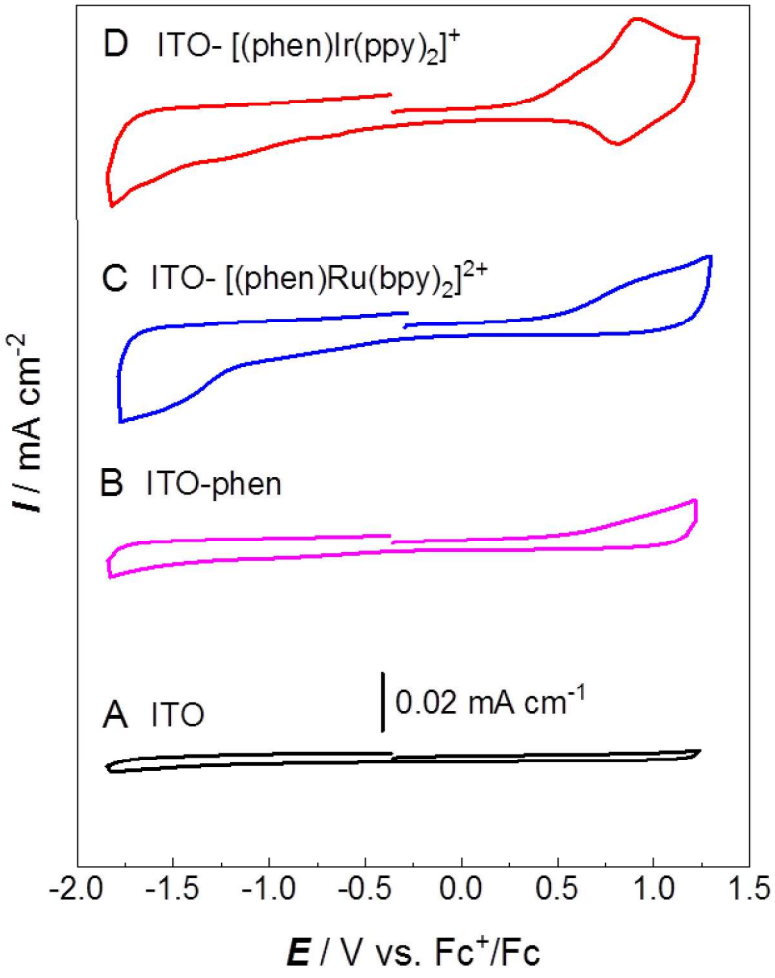

Figure 2. Cyclic voltammograms of the ITO electrodes throughout the chromophore grafting process in a N2-saturated CH2Cl2 solution containing 0.1 M NBu4PF6, scan rate: 200 mV s-1. (A) A bare ITO electrode, (B) an ITO-phen electrode, (C) an ITO-[(phen)Ru(bpy)2]2+ electrode, and (D) an ITO-[(phen)Ir(ppy)2]+ electrode.

279x361mm (300 x 300 DPI)

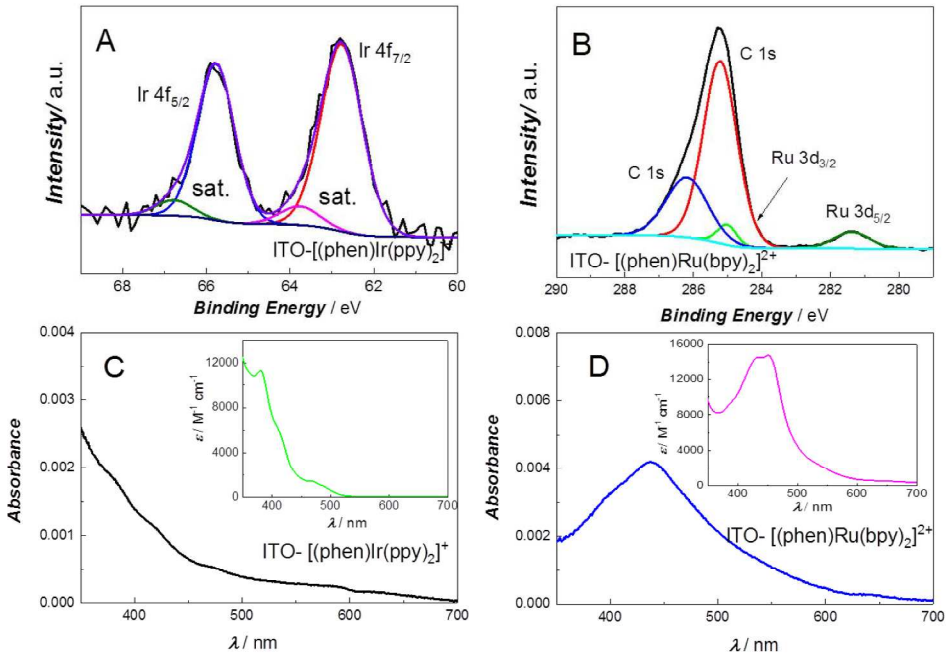

Figure 3. High resolution XPS spectra on (A) Ir 4f region of ITO-[(phen)Ir(ppy)2]+ electrode and (B) Ru 3d region of ITO-[(phen)Ru(bpy)2]2+ electrode. UV-vis absorption spectra of the (C) ITO-[(phen)Ir(ppy)2]+ and (D) ITO-[(phen)Ru(bpy)2]2+ electrodes with ITO absorbance deducted. The insets correspond to the UV-vis absorption spectra of the cis-[Ir(ppy)2(phen)] OTf and [Ru(bpy)2(phen)] (OTf)2 in CH2Cl2 solution, respectively.

297x210mm (300 x 300 DPI)

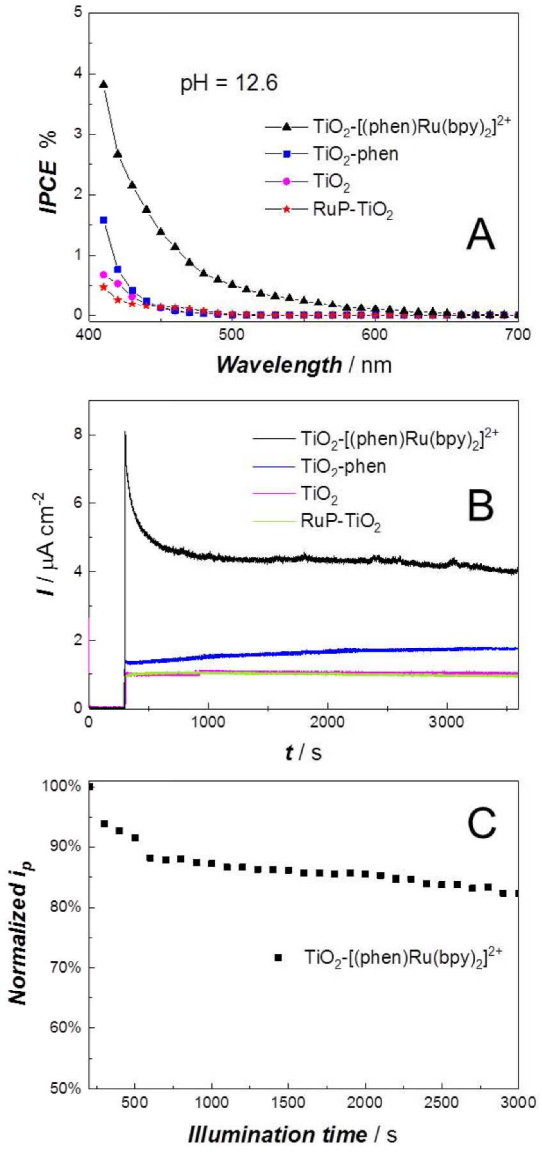

Figure 4. (A) The IPCE measurements and (B) Photoelectrochemical responses of the TiO2-[(phen)Ru(bpy)2]2+, TiO2-phen, bare TiO2 and RuP-TiO2 electrodes in 0.1 M NaClO4 containing 0.5 M triethylamine at constant potential of -0.3 V under Ar (pH = 12.6); (C) Photocurrent normalized to current at 200 s illumination for TiO2-[(phen)Ru(bpy)2]2+ electrode.

279x570mm (300 x 300 DPI)

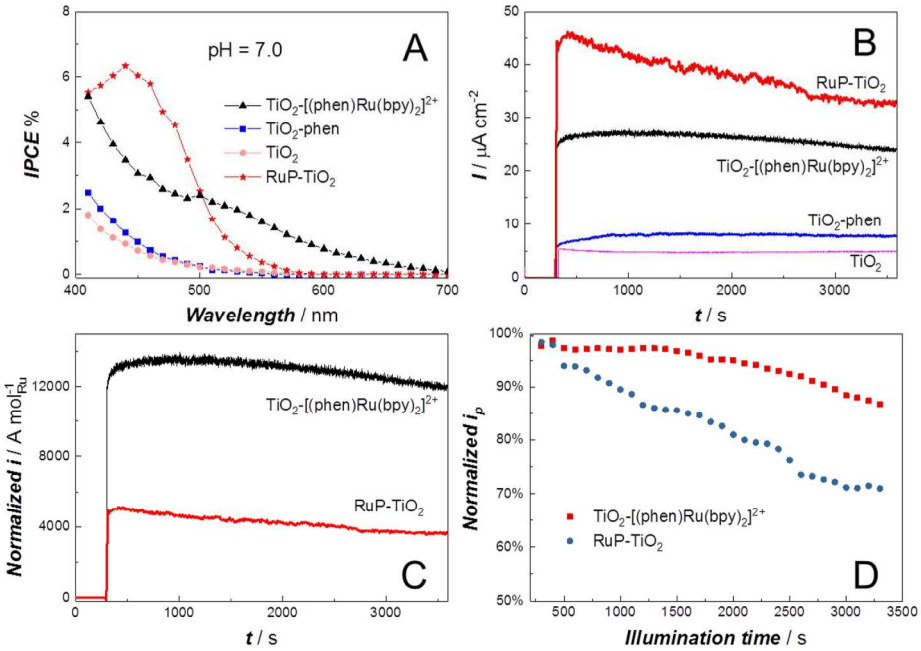

Figure 5. (A) The IPCE measurements and (B) Photoelectrochemical responses of TiO2-[(phen)Ru(bpy)2]2+, TiO2-phen, bare TiO2 and RuP-TiO2 electrodes in 0.1 M NaClO4 with 0.02 M hydroquinone under Ar at 0 V; (C) Photocurrent response normalized to moles of surface Ru for TiO2-[(phen)Ru(bpy)2]2+ and RuP-TiO2 electrodes in 0.1 M NaClO4 with 0.02 M hydroquinone under Ar at 0 V; (D) Photocurrent stability comparison between TiO2-[(phen)Ru(bpy)2]2+ and RuP-TiO2 normalized to the 200 s illumination current for each electrode. All solutions are stirred at 500 rpm.

215x166mm (300 x 300 DPI)

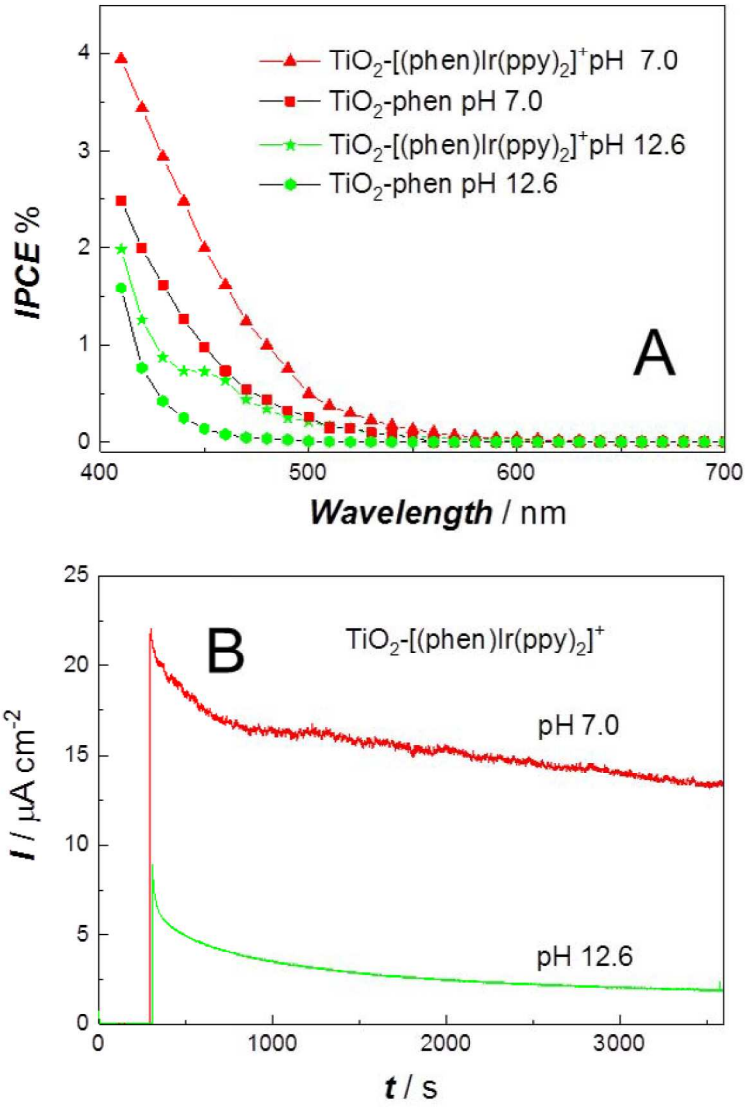

Figure 6. (A) The IPCE measurements and (B) Photoelectrochemical responses of the TiO2-[(phen)Ir(ppy)2]+ and TiO2-phen electrodes in 0.1 M NaClO4 containing 0.5 M triethylamine (pH = 12.6) at constant potential of -0.3 V, and in 0.1 M NaClO4 with 0.02 M hydroquinone (pH = 7.0) at 0 V under Ar. All the solutions are stirred at 500 rpm.

210x297mm (300 x 300 DPI)